

# Cosmological parameters degeneracies and non-Gaussian halo bias

---

**Carmelita Carbone**

*Dipartimento di Astronomia, Università di Bologna  
Via Ranzani 1, I-40127 Bologna, Italy  
E-mail: carmelita.carbone@unibo.it*

**Olga Mena**

*Depto. de Física Teórica, IFIC, Universidad de Valencia-CSIC  
Edificio de Institutos de Paterna, Apt. 22085, 46071 Valencia, Spain  
E-mail: omena@ific.uv.es*

**Licia Verde**

*ICREA & Instituto de Ciencias del Cosmos, Universitat de Barcelona  
Martí i Franques 1, 08028, Barcelona, Spain  
E-mail: liciaverde@icc.ub.edu*

**ABSTRACT:** We study the impact of the cosmological parameters uncertainties on the measurements of primordial non-Gaussianity through the large-scale non-Gaussian halo bias effect. While this is not expected to be an issue for the standard  $\Lambda$ CDM model, it may not be the case for more general models that modify the large-scale shape of the power spectrum. We consider the so-called local non-Gaussianity model, parametrized by the  $f_{\text{NL}}$  non-Gaussianity parameter which is zero for a Gaussian case, and make forecasts on  $f_{\text{NL}}$  from planned surveys, alone and combined with a Planck CMB prior. In particular, we consider EUCLID- and LSST-like surveys and forecast the correlations among  $f_{\text{NL}}$  and the running of the spectral index  $\alpha_s$ , the dark energy equation of state  $w$ , the effective sound speed of dark energy perturbations  $c_s^2$ , the total mass of massive neutrinos  $M_\nu = \sum m_\nu$ , and the number of extra relativistic degrees of freedom  $N_\nu^{\text{rel}}$ . Neglecting CMB information on  $f_{\text{NL}}$  and scales  $k > 0.03h/\text{Mpc}$ , we find that, if  $N_\nu^{\text{rel}}$  is assumed to be known, the uncertainty on cosmological parameters increases the error on  $f_{\text{NL}}$  by 10 to 30% depending on the survey. Thus the  $f_{\text{NL}}$  constraint is remarkable robust to cosmological model uncertainties. On the other hand, if  $N_\nu^{\text{rel}}$  is simultaneously constrained from the data, the  $f_{\text{NL}}$  error increases by  $\sim 80\%$ . Finally, future surveys which provide a large sample of galaxies or galaxy clusters over a volume comparable to the Hubble volume can measure primordial non-Gaussianity of the local form with a marginalized  $1-\sigma$  error of the order  $\Delta f_{\text{NL}} \sim 2 - 5$ , after combination with CMB priors for the remaining cosmological parameters. These results are competitive with CMB bispectrum constraints achievable with an ideal CMB experiment.

**KEYWORDS:** cosmology: theory, large-scale structure of universe – galaxies: clusters, general – galaxies: halos.

---

## Contents

<b>1. Introduction</b>	<b>1</b>
<b>2. Non-Gaussian halo bias</b>	<b>2</b>
<b>3. Methodology</b>	<b>4</b>
<b>4. Model parameters</b>	<b>6</b>
<b>5. Results</b>	<b>10</b>
<b>6. Conclusions</b>	<b>12</b>

---

## 1. Introduction

Tests of deviations from Gaussian initial conditions offer an important window into the very early Universe and a powerful test for the mechanism which generated primordial perturbations. While standard single-field slow-roll models of inflation lead to small departures from Gaussianity, non-standard scenarios allow for a larger non-Gaussianity (NG) level (e.g. [1, 2, 3], and refs. therein).

In particular, large NG can be produced if any of the conditions below is violated: *a*) single field, *b*) canonical kinetic energy *c*) slow roll and *d*) adiabatic (Bunch-Davies) initial vacuum state. The type of NG arising in standard inflation reads [4, 5, 6, 7]

$$\Phi = \phi + f_{\text{NL}} (\phi^2 - \langle \phi^2 \rangle) , \quad (1.1)$$

where  $\Phi$  denotes Bardeen's gauge-invariant potential, which, on sub-Hubble scales reduces to the usual Newtonian peculiar gravitational potential up to a minus sign, and  $\phi$  denotes a Gaussian random field. The NG parameter  $f_{\text{NL}}$  is often considered to be a constant, yielding NG of the *local* type with a bispectrum which is maximized for squeezed configurations [8]. NG of the local type is generated in standard inflationary scenarios (where  $f_{\text{NL}}$  is expected to be of the same order of the slow-roll parameters) as well as in multi-field inflationary scenarios<sup>1</sup>.

The standard observables to constrain NG are the Cosmic Microwave Background (CMB) and the Large-Scale Structure (LSS) of the Universe. Traditionally, the most

---

<sup>1</sup>Note that Eq. (1.1) is not general, i.e. there is a plethora of possible deviations from Gaussianity arising in the different inflationary scenarios proposed in the literature.

popular method to detect primordial NG has been to measure the bispectrum or the three-point correlation function of the CMB [6, 9, 10], while the LSS bispectrum has been shown to be sensitive to primordial NG only at high redshift [6, 11, 12, 13, 14].

Other powerful techniques to measure NG are based on weak lensing tomography [15], Integrated Sachs-Wolfe effect (ISW) [16, 17], abundance [18, 19, 20, 21, 22] and clustering [23, 24] of rare events such as density peaks, since they trace the tail of the underlying distribution.

Refs. [25] and [26] (hereafter MV08) showed that primordial NG affects the clustering of dark matter halos inducing a scale-dependent large-scale bias. This effect, which goes under the name of non-Gaussian halo bias, is particularly promising, yielding already stringent constraints from existing data [27, 17]. Forthcoming constraints on NG exploiting the non-Gaussian halo bias are expected to be similar to those achievable from an ideal CMB survey [16]. These predictions have been confirmed by N-body simulations [25, 28, 29, 30].

Forecasts for  $f_{\text{NL}}$  constraints from the halo-bias have been carried out so far assuming perfect knowledge of all other cosmological parameters. While for a  $\Lambda$ CDM model this is expected to be a reasonable assumption, for more general models one may expect  $f_{\text{NL}}$  to be degenerate with other parameters and thus to have a larger marginal error. Here we study the degeneracies among the large-scale non-Gaussian halo bias (for NG of the local type) and the cosmological parameters which affect the large-scale halo power spectrum, focusing on dark energy perturbations, massive neutrinos, number of relativistic species, and running spectral index, which can produce large deviations of the underlying cosmology from the minimal  $\Lambda$ CDM scenario. The paper is organized as follows. In §2 we briefly review the analytic expressions of the non-Gaussian halo power spectrum generalized to redshift dependent transfer functions. The redshift dependence is due to the presence of both dark energy perturbations and massive neutrinos. In §3 we summarize the Fisher matrix formalism applied to the observed halo power spectrum. In §4 we describe the assumed fiducial cosmology. Finally, in §5 and §6 we discuss the results and draw our conclusions.

## 2. Non-Gaussian halo bias

Here we summarize the derivation of [26], extending it to the case of a redshift dependent transfer function. In Fourier space, the filtered linear over-density  $\delta_R$  is related to the primordial potential  $\Phi(\mathbf{k})$  by the Poisson equation:

$$\delta_R(\mathbf{k}, z) = \frac{2}{3} \frac{D(z)T(k, z)k^2 c^2}{H_0^2 \Omega_{m,0}} W_R(k) \Phi(\mathbf{k}) \equiv \mathcal{M}_R(k, z) \Phi(\mathbf{k}) , \quad (2.1)$$

where  $T(k, z)$  denotes the matter transfer function (which is redshift dependent in the presence of massive neutrinos and/or dark energy perturbations),  $W_R(k)$  is the Fourier transform of the top-hat function of width  $R$ ,  $H_0$  and  $\Omega_{m,0}$  are the current values of the Hubble constant and the total matter energy density respectively, and  $D(z) = (1 +$

$z)^{-1}g(z)/g(0)$  is the linear growth-factor of density fluctuations, normalized to  $D(0) = 1$  with  $g(z)$  being the growth suppression factor for non Einstein-de Sitter universes.

In this context, the non-Gaussian halo power-spectrum takes the form

$$P_h(k, z) = b_{L,h}^2(z, M)P_{\delta\delta}(k, z) [1 + 4f_{\text{NL}}b_{L,h}(z, M)\beta(k, z)]. \quad (2.2)$$

Here  $b_{L,h}(z, M) \equiv q\delta_c(z)/(\sigma_M^2 D(z))$  is the Gaussian lagrangian bias<sup>2</sup> for dark matter halos of mass  $M$  [34],  $\sigma_M^2$  is the mass variance linearly extrapolated to  $z = 0$ ,  $\delta_c(z) \equiv \Delta_c(z)/D(z)$ , being  $\Delta_c(z)$  the linear overdensity for spherical collapse, which can be considered as a constant  $\Delta_c(z) = 1.686$ , even in the presence of dark energy [35],  $q$  is a factor extracted from N-body simulations ([28] and references therein) and  $P_{\delta\delta}(k, z)$  is the power spectrum of  $\delta_R$  (as it will be shown later in Eq. (4.8)). Finally,  $\beta(k, z)$  is defined as

$$\beta(k, z) \equiv \frac{1}{8\pi^2 \mathcal{M}_R(k, z)} \int dk_1 k_1^2 \mathcal{M}_R(k_1, z) P_\phi(k_1) \int_{-1}^1 d\mu \mathcal{M}_R(\sqrt{\alpha}, z) \left[ \frac{P_\phi(\sqrt{\alpha})}{P_\phi(k)} + 2 \right], \quad (2.3)$$

where  $\alpha = k_1^2 + k^2 + 2k_1 k \mu$ . Here we adopt the so-called CMB  $f_{\text{NL}}$  normalization where Eq. (1.1) is intended to be deep in the matter-dominated era<sup>3</sup>. Consequently, the non-Gaussian halo Lagrangian bias reads<sup>4</sup>

$$b_{L,h}^{\text{NG}}(z, M) \simeq b_{L,h}(z, M) [1 + 2f_{\text{NL}}b_{L,h}(z, M)\beta(k, z)]. \quad (2.4)$$

Making the standard assumption that halos move coherently with dark matter, the Eulerian bias is  $b_E = 1 + b_L$ . The halo power spectrum given by Eq. (2.2), is connected directly to the underlying dark matter power spectrum and can be reconstructed from the galaxy power spectrum using different techniques (e.g. [39]). It provides important information on the growth of structure, which helps in constraining dark energy and neutrino masses together with primordial non-Gaussianities. We shall exploit information from both the shape and the amplitude of the NG halo power spectrum up to scales  $k < 0.03h/\text{Mpc}$ , where  $\beta(k, z)$  has a negligible dependence on the halo mass (recall that for local non-Gaussianity  $\beta(k, z) \propto 1/k^2$ ). In addition, Eqs. (2.2)-(2.4) are valid only on scales much larger than the Lagrangian radius of the halo [26, 16] and have been tested and calibrated on N-body simulations only on scales  $k < 0.03h/\text{Mpc}$  [28]. We believe that the approach followed here is conservative, since in our parameter forecasts we do not consider scales  $k > 0.03h/\text{Mpc}$  in the halo power spectrum, which could provide much tighter constraints on cosmology, via e.g. Baryonic Acoustic Oscillations (BAO). In what follows, we shall use Eq. (2.2) to propagate errors of the non-Gaussian halo power spectrum into errors of the cosmological parameters via a Fisher matrix approach, as described below.

---

<sup>2</sup>In general, the Gaussian halo bias may have a non trivial dependence on both the halo formation redshift  $z_f$  and the observation redshift  $z_o$  [31, 32, 33]. However, for objects that did not undergo recent mergers,  $z_f \gg z_o$ , or in the case of rapid mergers  $z_f \approx z_o$  for  $\delta_c^2 \gg \sigma_M^2$ , i.e. large  $M$  and/or high  $z_f$ , the bias is well approximated by Eq. (2.2).

<sup>3</sup>See [28] for the large-scale structure-normalized conversions.

<sup>4</sup>A more accurate expression is given by  $b_{L,h}^{\text{NG}}(z, M) = b_{L,h}(z, M)\sqrt{1 + 4f_{\text{NL}}b_{L,h}(z, M)\beta(k, z)}$

### 3. Methodology

In this paper we adopt the Fisher matrix formalism to make predictions of the cosmological parameter errors including the NG parameter  $f_{\text{NL}}$ . The Fisher matrix is defined as the second derivative of the likelihood surface about the maximum. As long as the posterior distribution for the parameters is well approximated by a multivariate Gaussian function, its elements are given by [40, 41, 42]

$$F_{\alpha\beta} = \frac{1}{2} \text{Tr} [C^{-1} C_{,\alpha} C^{-1} C_{,\beta}] , \quad (3.1)$$

where  $C = S + N$  is the total covariance which consists of signal  $S$  and noise  $N$  terms. The commas in Eq. (3.1) denote derivatives with respect to the cosmological parameters within the assumed fiducial cosmology<sup>5</sup>.

To derive realistic parameter forecasts, we consider future redshift surveys, as Euclid<sup>6</sup>- and LSST<sup>7</sup>-like galaxy surveys. While for BAO surveys an accurate redshift measurement is crucial [43, 44], for our purposes, a precise redshift extraction is not needed, as it will be explained after Eq. (3.3). For the EUCLID-like survey we will assume a redshift coverage of  $0.5 < z < 2$  and a sky area of  $f_{\text{sky}} = 20000 \text{ deg}^2$ . For the LSST-like survey, we will consider  $0.3 < z < 3.6$  and  $f_{\text{sky}} = 30000 \text{ deg}^2$  for redshift and area coverages, respectively. In order to explore the cosmological parameters constraints from a given redshift survey, it is mandatory to specify the measurement uncertainties of the halo power spectrum. In general, the statistical error on the measurement of  $P_{\text{h}}(k)$  at a given wavenumber bin is given by [45]

$$\left[ \frac{\Delta P_{\text{h}}}{P_{\text{h}}} \right]^2 = \frac{2(2\pi)^2}{V k^2 \Delta k \Delta \mu} \left[ 1 + \frac{1}{\bar{n}_{\text{h}} P_{\text{h}}} \right]^2 , \quad (3.2)$$

where  $\bar{n}_{\text{h}}$  is the mean number density of dark matter halos,  $V$  is the comoving survey volume of the galaxy survey, and  $\mu$  is the cosine of the angle between  $\mathbf{k}$  and the line-of-sight direction.

To our purposes it is adequate to perform an angular average over  $\mu$ . Thus, our Fisher matrix for the large-scale structure data is given by

$$F_{\alpha\beta}^{\text{LSS}} = 2 \frac{V}{8\pi^2} \int_{k_{\text{min}}}^{k_{\text{max}}} k^2 dk \frac{\partial \ln P_{\text{h}}(k)}{\partial p_{\alpha}} \frac{\partial \ln P_{\text{h}}(k)}{\partial p_{\beta}} \left[ \frac{\bar{n}_{\text{h}} P_{\text{h}}(k)}{\bar{n}_{\text{h}} P_{\text{h}}(k) + 1} \right]^2 , \quad (3.3)$$

where  $p_{\alpha}$  represents the chosen set of cosmological parameters.

We divide the surveys in redshift bins of width  $\Delta z = 0.1$  (larger than standard photometric and spectroscopic redshift errors), and set  $k_{\text{max}}$  to be  $0.03h/\text{Mpc}$  and  $k_{\text{min}}$  to be greater than  $2\pi/\Delta V^{1/3}$ , where  $\Delta V$  is the volume of the redshift shell. Conservatively, we

---

<sup>5</sup>In practice, it can happen that the choice of parameterization makes the posterior distribution slightly non-Gaussian. However, even in this case, the error introduced by assuming Gaussianity in the posterior distribution can be considered as reasonably small, and therefore the Fisher matrix approach still holds as an excellent approximation for parameter forecasts.

<sup>6</sup><http://sci.esa.int/euclid>

<sup>7</sup>[http://www.lsst.org/lsst/science/scientist\\_dark\\_energy](http://www.lsst.org/lsst/science/scientist_dark_energy)

do not consider here that scales larger than  $k_{\min}$  can be used by cross-correlating different shells.

The effect of NG alters the broad-band behavior of  $P_h(k)$  on very large scales, where  $P_h(k)$  is unaffected by the precision with which the radial positions of the galaxies are measured. Thus, we can treat photometric and spectroscopic surveys on the same footing. Moreover, the requirement of surveying a large volume of the universe and sampling highly biased galaxies to beat shot-noise, which is a key point for BAO surveys, is also a bonus for constraining primordial NG [16].

Note, moreover, that the NG correction of the halo bias is boosted by the Lagrangian Gaussian halo bias factor itself.

In particular, for the value of  $k_{\min}$  used here, we find that  $P_h(k_{\min}) \simeq P_h(k = 0.2h/\text{Mpc})$ , thus, the shot-noise requirement for BAO surveys of  $\bar{n}P(k = 0.2h/\text{Mpc}) > 1$ , implies that for all scales of interest here,  $\bar{n}P \gg 1$ . We have checked that our results do not change if we impose  $\bar{n}P \sim 3$  at all scales.

We compute as well the CMB Fisher matrix to obtain forecasts for the Planck satellite<sup>8</sup>. We follow here the method of [46], considering the likelihood function for a realistic experiment with partial sky coverage, and noisy data

$$\begin{aligned}
-2 \ln \mathcal{L} = \sum_{\ell} (2\ell + 1) & \left\{ f_{\text{sky}}^{BB} \ln \left( \frac{\mathbf{C}_{\ell}^{BB}}{\hat{\mathbf{C}}_{\ell}^{BB}} \right) + \sqrt{f_{\text{sky}}^{TT} f_{\text{sky}}^{EE}} \ln \left( \frac{\mathbf{C}_{\ell}^{TT} \mathbf{C}_{\ell}^{EE} - (\mathbf{C}_{\ell}^{TE})^2}{\hat{\mathbf{C}}_{\ell}^{TT} \hat{\mathbf{C}}_{\ell}^{EE} - (\hat{\mathbf{C}}_{\ell}^{TE})^2} \right) \right. \\
& \left. + \sqrt{\frac{f_{\text{sky}}^{TT} f_{\text{sky}}^{EE}}{f_{\text{sky}}^{TT} f_{\text{sky}}^{EE}}} \frac{\hat{\mathbf{C}}_{\ell}^{TT} \mathbf{C}_{\ell}^{EE} + \mathbf{C}_{\ell}^{TT} \hat{\mathbf{C}}_{\ell}^{EE} - 2\hat{\mathbf{C}}_{\ell}^{TE} \mathbf{C}_{\ell}^{TE}}{\mathbf{C}_{\ell}^{TT} \mathbf{C}_{\ell}^{EE} - (\mathbf{C}_{\ell}^{TE})^2}} + f_{\text{sky}}^{BB} \frac{\hat{\mathbf{C}}_{\ell}^{BB}}{\mathbf{C}_{\ell}^{BB}} - 2\sqrt{f_{\text{sky}}^{TT} f_{\text{sky}}^{EE}} - f_{\text{sky}}^{BB} \right\} \quad (3.4)
\end{aligned}$$

and compute its second derivatives to obtain the corresponding Fisher matrix

$$F_{\alpha\beta}^{\text{CMB}} = \left\langle -\frac{\partial^2 L}{\partial p_{\alpha} \partial p_{\beta}} \right\rangle \Big|_{\mathbf{p}=\bar{\mathbf{p}}}. \quad (3.5)$$

In Eq. (3.4)  $\mathbf{C}_{\ell}^{XY} = \mathcal{C}_{\ell}^{XY} + \mathcal{N}_{\ell}^{XY}$  being  $\mathcal{C}_{\ell}^{XY}$  the temperature and polarization power spectra ( $X, Y \equiv \{T, E, B\}$ ) and  $\mathcal{N}_{\ell}$  the noise bias. Finally,  $f_{\text{sky}}^{XY}$  is the fraction of observed sky which can be different for the  $T$ -,  $E$ -, and  $B$ -modes. In Eq. (3.5)  $L \equiv \ln \mathcal{L}$ ,  $p_{\alpha}$  and  $p_{\beta}$  denote the cosmological parameters of the assumed model and form the vector  $\mathbf{p}$  whose fiducial value is given by  $\bar{\mathbf{p}}$ .

Combining the Planck and redshift survey Fisher matrices ( $F_{\alpha\beta} = F_{\alpha\beta}^{\text{LSS}} + F_{\alpha\beta}^{\text{CMB}}$ ) we get the joint constraints for  $\mathbf{p}$ . The  $1\text{-}\sigma$  error on  $p_{\alpha}$  marginalized over the other parameters is  $\sigma(p_{\alpha}) = \sqrt{(F^{-1})_{\alpha\alpha}}$ , being  $F^{-1}$  the inverse of the Fisher matrix. We then consider joint constraints in a two-parameter subspace (marginalized over all other cosmological parameters) to study the covariance between  $f_{\text{NL}}$  and the other cosmological parameters considered in this work.

Furthermore, in order to quantify the level of degeneracy between different parameters and  $f_{\text{NL}}$ , we estimate the so-called correlation coefficients, given by

$$r \equiv \frac{(F^{-1})_{p_{f_{\text{NL}}} p_{\alpha}}}{\sqrt{(F^{-1})_{p_{f_{\text{NL}}} p_{f_{\text{NL}}}} (F^{-1})_{p_{\alpha} p_{\alpha}}}}, \quad (3.6)$$

---

<sup>8</sup>[www.rssd.esa.int/PLANCK](http://www.rssd.esa.int/PLANCK)

where  $p_\alpha$  denotes one of the model parameters. When the coefficient  $|r| = 1$ , the two parameters are totally degenerate, while  $r = 0$  means they are uncorrelated.

**Table 1:** Correlation coefficients for  $M_\nu$ -cosmology

		$\Omega_b h^2$	$h$	$\Omega_{c,0} h^2$	$\Delta_{\mathcal{R}}^2(k_0)$	$n_s$	$w$	$c_s^2$	$\alpha_s$	$M_\nu$
LSST	$f_{\text{NL}}$	0.50	0.31	0.36	0.35	-0.03	0.41	-0.32	-0.31	0.03
LSST+Planck	$f_{\text{NL}}$	-0.22	-0.19	0.36	-0.12	0.14	-0.07	0.10	-0.13	0.34
EUCLID	$f_{\text{NL}}$	0.55	0.25	0.31	0.36	-0.06	0.39	-0.30	-0.24	0.09
EUCLID+Planck	$f_{\text{NL}}$	-0.17	-0.05	0.24	-0.07	0.06	-0.07	0.09	-0.05	0.16

**Table 2:** Correlation coefficients for  $N_\nu^{\text{rel}}$ -cosmology

		$\Omega_{b,0} h^2$	$h$	$\Omega_{c,0} h^2$	$\Delta_{\mathcal{R}}^2(k_0)$	$n_s$	$w$	$c_s^2$	$\alpha_s$	$N_\nu^{\text{rel}}$
LSST	$f_{\text{NL}}$	-0.06	0.34	0.12	-0.13	0.12	0.34	-0.39	-0.44	-0.64
LSST+Planck	$f_{\text{NL}}$	0.24	-0.48	0.61	-0.24	0.19	0.54	0.04	-0.08	0.69
EUCLID	$f_{\text{NL}}$	-0.05	0.34	0.08	-0.20	0.05	0.11	-0.26	-0.45	-0.69
EUCLID+Planck	$f_{\text{NL}}$	0.34	-0.57	0.76	-0.26	0.21	0.64	0.08	-0.05	0.77

#### 4. Model parameters

The Fisher matrix approach propagates errors of the observed  $P_h$ , see Eq. (3.2), into errors of the cosmological parameters which characterize the underlying fiducial cosmology. According to the latest observations (e.g. [51] and refs. therein), our fiducial  $\Lambda$ CDM cosmological parameters are:  $\Omega_{m,0} h^2 = 0.1358$ ,  $\Omega_{b,0} h^2 = 0.02267$ ,  $h = 0.705$ ,  $\Delta_{\mathcal{R}}^2(k_0) = 2.64 \times 10^{-9}$ ,  $n_s = 0.96$ ,  $\alpha_s = 0$  and  $f_{\text{NL}} = 0$ . Here  $\Omega_{m,0}$  and  $\Omega_{b,0}$  are the total matter and baryon present-day energy densities, respectively, in units of the critical energy density of the Universe,  $h$  is given by  $H_0 = 100h \text{ km s}^{-1} \text{ Mpc}^{-1}$ , where  $H_0$  is the Hubble constant,  $\Delta_{\mathcal{R}}^2(k_0)$  represents the dimensionless amplitude of the primordial curvature perturbations evaluated at a pivot scale  $k_0$ ,  $n_s$  is the scalar spectral index of the primordial matter power spectrum, assumed to be a power-law, and  $\alpha_s$  is the running of the scalar spectral index. We will consider two different fiducial models matching this  $\Lambda$ CDM cosmology as follows. We adopt the same values for the 7 “base” parameters. We do not consider primordial gravitational waves and assume a flatness prior,  $\Omega_K = 0$ , as predicted by long-lasting inflation models, so that  $\Omega_{de,0} = 1 - \Omega_{m,0}$ , where  $\Omega_K$  and  $\Omega_{de,0}$  are, respectively,

**Table 3:**  $f_{\text{NL}}$  1- $\sigma$  errors for  $M_\nu$ -cosmology

fixed parameter	LSST	LSST+PLANCK	EUCLID	EUCLID+PLANCK
non-marginalized	1.65	1.65	2.79	2.79
marginalized	4.52	2.11	8.86	3.12
$\Omega_{b,0}h^2$	3.91	2.06	7.41	3.07
$h$	4.29	2.07	8.58	3.11
$\Omega_{c,0}h^2$	4.22	1.97	8.43	3.02
$\Delta_{\mathcal{R}}^2(k_0)$	4.22	2.10	8.27	3.11
$n_s$	4.52	2.09	8.85	3.11
$w$	4.12	2.11	8.16	3.11
$c_s^2$	4.27	2.10	8.44	3.11
$\alpha_s$	4.30	2.10	8.61	3.11
$M_\nu$	4.52	1.99	8.83	3.08
$\alpha_s, c_s^2$	4.05	2.09	8.13	3.10
$\alpha_s, M_\nu$	4.28	1.94	8.57	3.07
$c_s^2, M_\nu$	4.26	1.97	8.35	3.06
$c_s^2, M_\nu, \alpha_s$	4.02	1.93	8.03	3.06

**Table 4:**  $f_{\text{NL}}$  1- $\sigma$  errors for  $N_\nu^{\text{rel}}$ -cosmology

fixed parameter	LSST	LSST+PLANCK	EUCLID	EUCLID+PLANCK
non-marginalized	1.46	1.46	2.56	2.56
marginalized	5.08	2.56	10.15	4.79
$\Omega_{b,0}h^2$	5.07	2.49	10.13	4.51
$h$	4.77	2.25	9.53	3.93
$\Omega_{c,0}h^2$	5.05	2.03	10.12	3.13
$\Delta_{\mathcal{R}}^2(k_0)$	5.04	2.49	9.94	4.62
$n_s$	5.05	2.51	10.13	4.68
$w$	4.78	2.16	10.09	3.67
$c_s^2$	4.69	2.56	9.79	4.77
$\alpha_s$	4.57	2.55	9.06	4.78
$N_\nu^{\text{rel}}$	3.88	1.86	7.32	3.06
$\alpha_s, c_s^2$	4.16	2.55	8.70	4.77
$\alpha_s, N_\nu^{\text{rel}}$	3.76	1.76	7.15	2.92
$c_s^2, N_\nu^{\text{rel}}$	3.57	1.86	7.15	3.05
$c_s^2, N_\nu^{\text{rel}}, \alpha_s$	3.43	1.76	6.95	2.91

the present-day energy densities associated to the spatial curvature and to the dark energy component of the Universe, in units of the critical density.



A Gaussian prior of 5% on the present-day Hubble’s constant  $H_0 = 100h \text{ km s}^{-1} \text{ Mpc}^{-1}$  is assumed, following the results of [52]. While this uncertainty is comparable to the one achieved by recent WMAP-7yr data<sup>9</sup> in the determination of  $H_0$  for the  $\Lambda$ CDM model [51], this information will improve, as expected, the parameter constraints on models different from the minimal  $\Lambda$ CDM model, such as models with dark energy perturbations, massive neutrinos and non-vanishing running of the spectral index.

We also consider dark energy to be a cosmic fluid with clustering properties on the Gpc scale, described by an equation of state that we assume to be constant

$$w \equiv \frac{p_{de}}{\rho_{de}} = w|_{\text{fid}} , \quad (4.1)$$

where  $p_{de}$  and  $\rho_{de}$  represent respectively the pressure and energy density of the dark energy fluid, and we assume a fiducial value  $w|_{\text{fid}} = -0.9$  which lies well within the current 95% C.L. limits on a constant dark energy equation of state parameter  $w$ . The dark energy fluid will be also described here by an effective sound speed  $c_s$  which parametrizes the transition between the smooth and clustered dark-energy regimes [47]

$$c_s^2 \equiv \frac{\delta p_{de}}{\delta \rho_{de}} , \quad (4.2)$$

with fiducial value  $c_s^2|_{\text{fid}} = 0.9$ . Dark energy perturbations will arise only if the dark energy equation of state parameter  $w$  is different from  $-1$ .

We assume the power spectrum of primordial curvature perturbations,  $P_{\mathcal{R}}(k)$ , to be

$$\Delta_{\mathcal{R}}^2(k) \equiv \frac{k^3 P_{\mathcal{R}}(k)}{2\pi^2} = \Delta_{\mathcal{R}}^2(k_0) \left( \frac{k}{k_0} \right)^{n_s - 1 + \frac{1}{2}\alpha_s \ln(k/k_0)} . \quad (4.3)$$

where  $k_0 = 0.002/\text{Mpc}$  and  $\Delta_{\mathcal{R}}^2(k_0)|_{\text{fid}} = 2.64 \times 10^{-9}$  [48].

The matter energy density  $\Omega_{m,0}$  includes the neutrino contribution when neutrinos are non-relativistic

$$\Omega_{m,0} = \Omega_{c,0} + \Omega_{b,0} + \Omega_{\nu,0} , \quad (4.4)$$

where  $\Omega_{\nu,0}$  is related to the sum of neutrino masses  $M_\nu \equiv \sum m_\nu$  as

$$\Omega_{\nu,0} = \frac{M_\nu}{93.8h^2 \text{ eV}} , \quad (4.5)$$

and the neutrino mass eigenstates are assumed to have a *degenerate* spectrum, i.e. the three neutrinos have the same mass.

We will constrain the following set of “baseline” parameters

$$p_\alpha = \{ \Omega_{b,0}h^2, h, \Omega_{c,0}h^2, \Delta_{\mathcal{R}}^2(k_0), n_s, w, c_s, \alpha_s, f_{\text{NL}} \} . \quad (4.6)$$

From here we specify two cosmological models:

---

<sup>9</sup><http://lambda.gsfc.nasa.gov/>

- $N_\nu^{\text{rel}}$ -cosmology, where neutrinos are effectively massless but the the number of relativistic species  $N_\nu^{\text{rel}}$  can deviate from the standard value  $N_\nu^{\text{rel}} = 3.04$ . In this case the fiducial value  $N_\nu^{\text{rel}}|_{\text{fid}} = 3.04$  is chosen, fixing  $M_\nu = \text{const} = 0$ .  $N_\nu^{\text{rel}}$  is given by the energy density associated to radiation

$$\Omega_{r,0} = \Omega_{\gamma,0} \left( 1 + 0.2271 N_\nu^{\text{rel}} \right) , \quad (4.7)$$

where  $\Omega_{\gamma,0} = 2.469 \times 10^{-5} h^{-2}$  is the present-day photon energy density parameter for  $T_{\text{cmb}} = 2.725$  K [49].

- $M_\nu$ -cosmology, where  $N_\nu^{\text{rel}}$  is fixed at the fiducial value and  $M_\nu$  is allowed to vary. In this case, being still consistent with current data [50, 51] we choose a fiducial value  $M_\nu|_{\text{fid}} = 0.3$  eV. This choice is motivated by the fact that for taking two-sided numerical derivatives, the fiducial  $M_\nu$  must be non-zero. It is well known that the error from cosmological observations on the neutrino mass depends somewhat on the fiducial mass chosen; from [53] we estimate that around a fiducial  $M_\nu = 0$  the error on  $M_\nu = 0$  would increase by less than 20%. As it will be clear from Sec. 5 the effect of this correction will be negligible on the  $f_{\text{NL}}$  error estimate. In addition most of the signal to constrain  $M_\nu$  from LSS surveys will come from smaller scales (not considered here).

At the CMB level, if neutrinos are still relativistic at the decoupling epoch,  $z \simeq 1090$ , i.e. if the mass of the heaviest neutrino specie is  $m_\nu < 0.58$  eV, massive neutrinos do not affect the CMB power spectra, except through the gravitational lensing effect [49], and, as a consequence, the dark energy equation of state  $w$  is not degenerate with the neutrino mass. However, the limit on the the sum of the neutrino masses degrades significantly when the dark energy equation of state is a function of redshift, if the amplitude of the galaxy spectrum is used for getting constraints on  $w$  and  $M_\nu$ , since dark energy and massive neutrinos both affect the growth rate of structures.

In this work, both massive neutrinos and clustering properties of the dark energy perturbations are considered. In this scenario, the growth function of the dark matter perturbations is scale-dependent, even at the linear level. The overall effect induces a redshift-dependent transfer function [54, 55, 56], and the power spectrum of the linear density field, smoothed on a sphere of radius  $R$ , takes the form

$$P_{\delta\delta}(k, z) = \frac{8\pi^2 c^4 k_0 \Delta_{\mathcal{R}}^2(k_0)}{25 H_0^4 \Omega_{m,0}^2} W_R^2(k) T^2(k, z) D^2(z) \left( \frac{k}{k_0} \right)^{n_s + \frac{1}{2} \alpha_s \ln(k/k_0)} , \quad (4.8)$$

where  $D(z)$  is the *scale independent* linear growth-factor defined in §2. The redshift-dependent transfer function  $T(k, z)$  is directly extracted from CAMB<sup>10</sup>[57] at each redshift  $z$ , in order to compute the Fisher matrix, given by Eq. (3.3), within each redshift bin.

Our analysis exploit exclusively the linear matter power spectrum, since we restrict ourselves to scales  $k \leq 0.03h/\text{Mpc}$ , where the details of the halo occupation distribution of

---

<sup>10</sup><http://camb.info/>

galaxies are irrelevant. We focus here on dark matter halos with mass  $\sim 10^{12}$ – $10^{13}$  (where the lower mass limit is relative to the highest redshift of the survey).

Notice as well that in our Fisher matrix analysis we do not add constraints on the  $f_{\text{NL}}$  parameter from CMB experiments, so that our forecasts on  $f_{\text{NL}}$  result exclusively from future redshift survey measurements of the dark matter halo power spectrum on scales  $k \leq 0.03h/\text{Mpc}$ , i.e. without including information from BAOs which will further reduce the forecasted errors and residual degeneracies. For all the reasons explained above, the results presented in the next section should be considered conservative.

## 5. Results

In this Section we present the predicted  $1$ - $\sigma$  marginalized errors of the  $f_{\text{NL}}$  parameter, and the  $f_{\text{NL}}$  covariance with the remaining cosmological parameters considered in our Fisher matrix analysis. We show forecasts both from LSST and EUCLID data only, as well as the expected errors after combining the results from these two experiments with Planck forecasted errors.

First of all, when considering forecasts from the redshift surveys alone, we expect that the  $f_{\text{NL}}$  parameter will be correlated with all cosmological parameters which affect the amplitude and shape of  $P_{\text{h}}(k)$  at scales  $k \leq 0.03h/\text{Mpc}$ . Tables 1-2 show the correlation  $r$  (see Eq. (3.6)) among  $f_{\text{NL}}$  and the other cosmological parameters  $p_{\alpha}$ . We expect  $w$  and  $f_{\text{NL}}$  to be correlated. In fact, at scales  $k \leq 0.03h/\text{Mpc}$ , an increase of  $w$  produces a trend on the matter power spectrum which is *opposite* to the one produced in  $P_{\text{h}}(k)$  by increasing  $f_{\text{NL}}$ . So the effect of positively increasing  $f_{\text{NL}}$  can be mimicked by a larger  $w$  (see Fig. 1).

Likewise,  $f_{\text{NL}}$  is correlated with  $\Omega_{b,0}h^2$ ,  $\Omega_{c,0}h^2$ , and  $M_{\nu}$ , since, on the scales considered, the larger these parameters are, the smaller the matter power spectrum is, and this competes with the rise of  $P_{\text{h}}(k)$  due to an increasing value of  $f_{\text{NL}}$ .

On the other hand,  $f_{\text{NL}}$  is negatively correlated with both the running of the scalar spectral index  $\alpha_s$  and the effective sound speed of dark energy perturbations  $c_s$ . In fact, if either  $\alpha_s$  or  $c_s$  increase, the matter power spectrum  $P_{\delta\delta}$  is modified in a very similar way to the halo power spectrum  $P_{\text{h}}(k)$  for a larger  $f_{\text{NL}}$  value. Consequently, the effect of a positively increasing  $f_{\text{NL}}$  can be mimicked by decreasing either  $\alpha_s$  or  $c_s$ . For what concerns the effective number of relativistic species, the  $f_{\text{NL}}-N_{\nu}^{\text{rel}}$  correlation is more complicated, as it depends on several factors. Naively, one would expect a positively correlation between these two parameters, since an increase in the number of relativistic particles should suppress the matter power spectrum, which can be compensated by increasing  $f_{\text{NL}}$ . However, since the redshift evolution of the halo bias is also modified in this situation, the correlation coefficient may change its sign.

When the Planck Fisher matrix information is added to the survey Fisher matrix, all degeneracies are either resolved or drastically reduced. In some cases, the correlation coefficient  $r$  can even change sign, see Tabs. 1-2. This change in the behavior of  $r$  arises either due to the presence of dominant parameter degeneracies affecting the CMB spectrum, or because of marginalization of a high-dimension parameter space down to two variables.

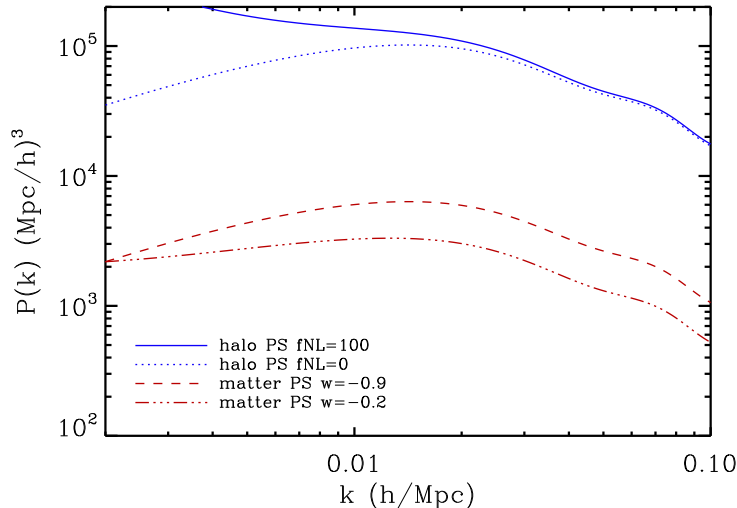


**Figure 1:** The solid blue line represents the NG halo power spectrum for  $f_{\text{NL}} = 100$  and halo mass  $M = 10^{13} M_{\odot}$ , while the dotted blue line is the corresponding Gaussian halo power spectrum ( $f_{\text{NL}} = 0$ ), at redshift  $z = 0$ . The dashed red line represents the matter power spectrum calculated for  $w = -0.9$ , while the red three-dot-dashed line is the matter power spectrum for  $w = -0.2$ . The matter power spectra are evaluated at  $z = 0$  and normalized to the same amplitude at  $k = 0.002$ . Note that  $\Delta(\ln P_h(k))/\Delta w$  and  $\Delta(\ln P_h(k))/\Delta f_{\text{NL}}$  have opposite sign in the range of  $k$  of interest here: it is clear from Eq. (3.3) that the two parameters can compensate each other, i.e. they are correlated

In particular, it is worth noting here that, while  $f_{\text{NL}}$  and  $N_{\nu}^{\text{rel}}$  are negatively correlated if only galaxy survey data are considered, they are positively correlated after adding Planck priors. In fact, since both  $N_{\nu}^{\text{rel}}$  and  $\Omega_{c,0} h^2$  are strongly, positively correlated at the CMB level via the equality redshift  $z_{\text{eq}}$ , then, a positive correlation between  $\Omega_{c,0} h^2$  and  $f_{\text{NL}}$  automatically turns into a correlation of the same sign between  $N_{\nu}^{\text{rel}}$  and  $f_{\text{NL}}$ . Despite the residual non-zero correlation coefficients, one should bear in mind that the marginalized  $f_{\text{NL}}$  errors decrease by a factor  $> 2$  when the CMB prior is added.

From our analysis, we conclude that the effective number of relativistic species is the main parameter affecting the constraints on  $f_{\text{NL}}$ .

The  $1-\sigma$  errors of  $f_{\text{NL}}$ , for the two fiducial cosmologies considered here, are shown in Tabs. 3 and 4. Let us notice that the marginalized errors are significantly larger than the non-marginalized ones when only the LSS surveys are used for the forecasts. Nonetheless, the marginalized errors become comparable in magnitude to the non-marginalized errors when Planck priors are added, since the CMB mitigates the intrinsic degeneracies between  $f_{\text{NL}}$  and the other cosmological parameters at the LSS level. It is also worth noting that the non-marginalized  $1-\sigma$  errors of  $f_{\text{NL}}$  presented in this work are larger than the corresponding errors presented in [16]. In fact we now consider less highly biased halos, with a fiducial bias parameter more in-line with the expected one for (blue) EUCLID galaxies [58, 59]. It

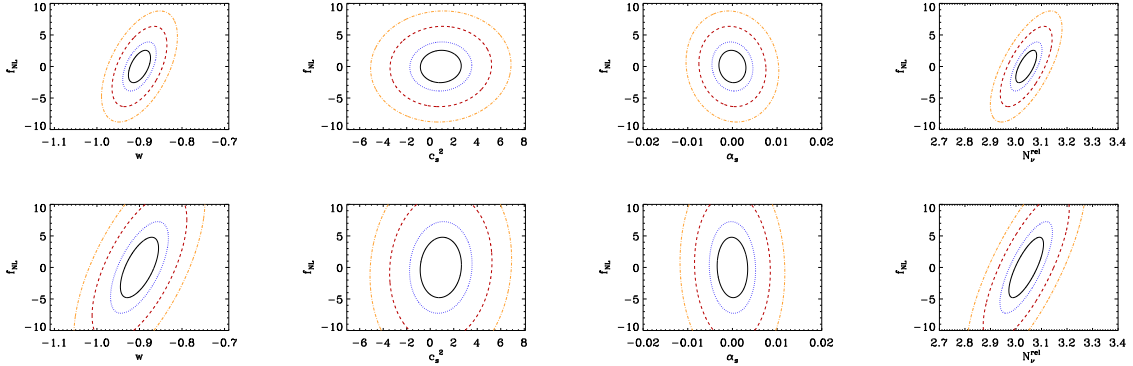


**Figure 2:** 2-parameter  $f_{\text{NL}}-p_\alpha$  joint contours for the fiducial model with extra relativistic degrees of freedom  $N_\nu^{\text{rel}}$  as described in the text, obtained after combining LSST (upper panels) and EUCLID (lower panels) data with Planck priors. The blue dotted line, the red dashed line and the orange dot-dashed line represent the 68% C.L., 95.4% C.L. and 99.73% C.L., respectively. The black solid line shows the 1-parameter confidence level at  $1-\sigma$ .

is important to note that the  $f_{\text{NL}}$  effect on the halo bias is modulated by  $b_{L,h}(z, M)$ , which depends crucially on the selected halo and its merging history [60, 61].

Tabs. 3-4 show as well the effect of each cosmological parameter on the  $f_{\text{NL}}$  forecasts. Obviously the parameters which have a larger impact on the  $f_{\text{NL}}$  errors are the ones more degenerated with it, and can be directly inferred from Tabs. 1-2. Moreover, since with the inclusion of the parameters  $\alpha_s$ ,  $c_s$ ,  $M_\nu$  and  $N_\nu^{\text{rel}}$ , we have considered cosmologies which deviate substantially from the minimal  $\Lambda$ CDM model, we fix pairs/triplets composed by these parameters to show how much deviations from a  $\Lambda$ CDM cosmology can affect the  $f_{\text{NL}}$  constraints. For the  $N_\nu^{\text{rel}}$  model cosmology there is an important impact on the  $f_{\text{NL}}$  marginalized errors from  $\Omega_{c,0}h^2$ ,  $h$ ,  $w$  and, in particular, from  $N_\nu^{\text{rel}}$ . In summary, if  $N_\nu^{\text{rel}}$  is assumed to be fixed, the uncertainties on the other cosmological parameters increase the error on  $f_{\text{NL}}$  only by 10 to 30%, depending on the survey. If  $N_\nu^{\text{rel}}$  is considered as an extra parameter to be simultaneously constrained from the data then the uncertainty in the underlying cosmology increases the  $f_{\text{NL}}$  error by  $\sim 80\%$ .

In Figs. 2-3 we show the 2-parameter projected 68% C.L., 95.4% C.L. and 99.73% C.L. contours in the  $f_{\text{NL}}-p_\alpha$  sub-space with  $p_\alpha = w, c_s^2, \alpha_s, M_\nu, N_\nu^{\text{rel}}$ , obtained after combining LSST and EUCLID data with Planck priors for the two fiducial models considered in this work. The black line shows the 1-parameter confidence level at  $1-\sigma$ . The orientation of the ellipses reflects the correlations among the parameters shown in Tabs. 1-2.

## 6. Conclusions

Deviations from non-Gaussianity, usually parameterized by the parameter  $f_{\text{NL}}$ , offer a powerful tool to identify the mechanism which generates the seeds for the structures we observe currently in our Universe.

Here we study the impact of the uncertainties of the cosmological parameters on the  $f_{\text{NL}}$  errors expected for the case of local non-Gaussianity for the large-scale non-Gaussian

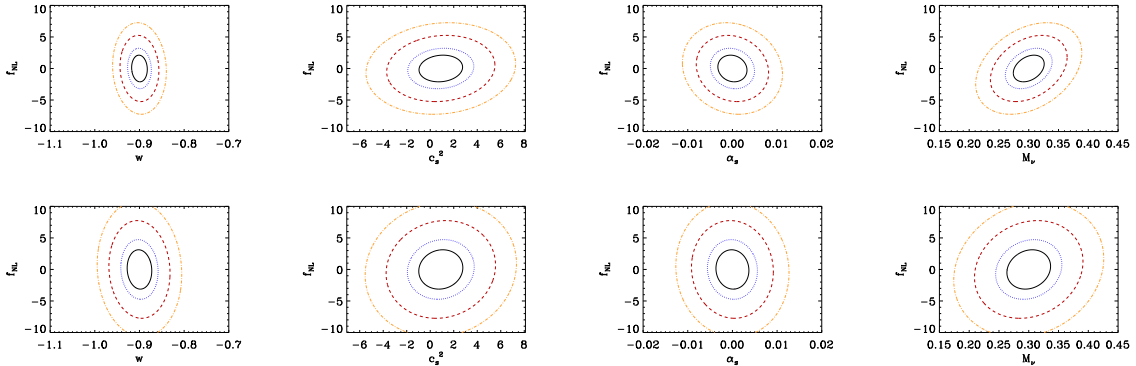


**Figure 3:** The same as in Fig. 2, for the fiducial model with massive neutrinos of total mass  $M_\nu|_{\text{fid}} = 0.3$  eV, as described in the text.

halo bias effect. We forecast the correlations among  $f_{\text{NL}}$  and the remaining cosmological parameters (including the running of the spectral index  $\alpha_s$ , and the dark energy parameters  $w$  and  $c_s^2$ ) within two possible cosmological models. The first model contains massive neutrinos (hypothesis robustly confirmed by neutrino oscillation data), where the total neutrino mass is a parameter to be constrained by the cosmological data. The second model assumes massless neutrinos (or neutrinos with a mass too small to be relevant for the cosmological observations considered here) and allows for extra relativistic degrees of freedom  $N_\nu^{\text{rel}}$ , which could be induced by the presence of sterile neutrinos, non minimally coupled quintessence fields, or even by the violation of the spin statistics theorem in the neutrino sector.

We follow here a conservative approach, assuming that  $f_{\text{NL}}$  is constrained exclusively from the very large scale halo power spectrum (i.e. we neglect CMB information on  $f_{\text{NL}}$ ), and restrict ourselves to scales  $k \leq 0.03h/\text{Mpc}$ , without exploiting information e.g., from BAOs, which will further reduce degeneracies and forecasted errors. We present first the Fisher matrix forecasts for  $f_{\text{NL}}$  assuming EUCLID- and LSST-like surveys for the two model cosmologies considered here. Then, we add the Planck Fisher forecasts for the remaining cosmological parameters to study the impact on the  $f_{\text{NL}}$  correlations.

The combined errors on  $f_{\text{NL}}$  do not change significantly in the presence of a dark energy equation of state, massive neutrinos, running of the spectral index, or clustering of dark energy perturbations, which are the parameters we have particularly focused on, since they are expected to affect the matter power spectrum on large scales, and represent the main deviations from a minimal  $\Lambda\text{CDM}$  model. However, the errors on  $f_{\text{NL}}$  are highly affected in the presence of extra relativistic degrees of freedom  $N_\nu^{\text{rel}}$ . We find that if  $N_\nu^{\text{rel}}$  is assumed to be fixed, the effect of the uncertainties on the other cosmological parameters increases the error on  $f_{\text{NL}}$  only by 10 to 30% depending on the survey. If  $N_\nu^{\text{rel}}$  is considered as a parameter to be simultaneously constrained from the data, then the uncertainty in the underlying cosmology increases the  $f_{\text{NL}}$  error by  $\sim 80\%$ . We thus conclude that, except for the effect of  $N_\nu^{\text{rel}}$ , the halo-bias  $f_{\text{NL}}$  constraints are remarkably robust to uncertainties in the underlying cosmology.

One important point to discuss is the effect of the (Gaussian) halo bias, as its value boosts the effect of  $f_{\text{NL}}$  on the halo power spectrum shape, and in our analysis it has been assumed to be known. The (Gaussian) halo bias depends strongly on the type of halos selected by the survey –whether they correspond to extremely high and rare peaks in the initial fluctuation field–, and on their accretion history. Errors on  $f_{\text{NL}}$  may be improved –at least in principle– by up to a factor of two by optimizing the choice of tracers.

The bias factor itself will need to be estimated from the survey, at the same time as the other cosmological parameters; the signal comes from scales much smaller than those used here, where the NG effect on halo bias is completely negligible. We estimate that the error on the (Gaussian) halo bias will be of the same order (in %) as the error on the linear growth factor  $f$  as a function of redshift, which is forecasted to be  $< \sim 10\%$  [62, 63]. Such a residual uncertainty will therefore increase the  $f_{\text{NL}}$  errors reported here by at most 10%.

Let us recall that the purpose of this work is to show the main correlations between  $f_{\text{NL}}$  and the other cosmological parameters, and to understand if these degeneracies can degrade dramatically the  $f_{\text{NL}}$  errors. We have shown that, after the combination with Planck constraints on parameters different from  $f_{\text{NL}}$ , the degeneracies get mostly broken, independently on the particular cosmological parameter, even without adding information from smaller scales corresponding to  $k > 0.03h/\text{Mpc}$ . Therefore we conclude that the  $f_{\text{NL}}$  constraints are very robust against underlying cosmology assumptions.

Finally, future surveys which provide a large sample of galaxies or galaxy clusters over a volume comparable to the Hubble volume (LSST, EUCLID) will measure primordial non-Gaussianity of the local form with a marginalized  $1\text{-}\sigma$  error of the order  $\Delta f_{\text{NL}} \sim 2\text{--}5$ , after combination with CMB priors for the remaining cosmological parameters. These results are competitive with CMB bispectrum constraints achievable with an ideal CMB experiment  $\Delta f_{\text{NL}} \sim \text{few}$  [64, 65].

## Acknowledgments

CC acknowledges the support from the Agenzia Spaziale Italiana (ASI, contract N. I/058/08/0). OM is supported by a Ramón y Cajal contract from the MICINN. LV is supported by FP7-PEOPLE-2007-4-3-IRG n. 202182 and FP7-IDEAS-Phys.LSS 240117. LV and OM are supported by the MICINN grant AYA2008-03531; LV acknowledges hospitality of Theory Group, Physics Department, CERN, and of Astronomy department of Università di Bologna, where part of the work was carried out.

## References

- [1] Bartolo, N., Komatsu, E., Matarrese, S., & Riotto, A. 2004, *Phys. Rep.*, 402, 103
- [2] Bartolo, N., Matarrese, S., & Riotto, A. 2005, *J. Cosm. Astropart. Phys.*, 10, 10
- [3] Chen, X. 2010, [arXiv:1002.1416](https://arxiv.org/abs/1002.1416), to appear in special issue of Advances in Astronomy on “Testing the Gaussianity and Statistical Isotropy of the Universe”
- [4] Salopek, D. S., & Bond, J. R. 1990, *Phys. Rev. D*, 42, 3936
- [5] Gangui, A., Lucchin, F., Matarrese, S., & Mollerach, S. 1994, *Astrophys. J.*, 430, 447

- [6] Verde, L., Wang, L., Heavens, A. F., & Kamionkowski, M. 2000, *Mon. Not. Roy. Astron. Soc.*, 313, 141
- [7] Komatsu, E., & Spergel, D. N. 2001, *Phys. Rev. D*, 63, 063002
- [8] Babich, D., Creminelli, P., & Zaldarriaga, M. 2004, *J. Cosm. Astropart. Phys.*, 8, 9
- [9] Komatsu, E., Spergel, D. N., & Wandelt, B. D. 2005, *Astrophys. J.*, 634, 14
- [10] Yadav, A. P. S., & Wandelt, B. D. 2008, *Phys. Rev. Lett.*, 100, 181301
- [11] Scoccimarro, R., Sefusatti, E., & Zaldarriaga, M. 2004, *Phys. Rev. D*, 69, 103513
- [12] Sefusatti, E., & Komatsu, E. 2007, *Phys. Rev. D*, 76, 083004
- [13] Cooray, A. 2006, *Phys. Rev. Lett.*, 97, 261301
- [14] Pillepich, A., Porciani, C., & Matarrese, S. 2007, *Astrophys. J.*, 662, 1
- [15] Fedeli, C., & Moscardini, L. 2009, [arXiv:0912.4112](https://arxiv.org/abs/0912.4112), *Mon. Not. Roy. Astron. Soc.* in press
- [16] Carbone, C., Verde, L., & Matarrese, S. 2008, *Astrophys. J.*, 684, L1
- [17] Afshordi, N., & Tolley, A. J. 2008, *Phys. Rev. D*, 78, 123507
- [18] Matarrese, S., Verde, L., & Jimenez, R. 2000, *Astrophys. J.*, 541, 10
- [19] Verde, L., Jimenez, R., Kamionkowski, M., & Matarrese, S. 2001, *Mon. Not. Roy. Astron. Soc.*, 325, 412
- [20] LoVerde, M., Miller, A., Shandera, S., & Verde, L. 2008, *J. Cosm. Astropart. Phys.*, 0804,014
- [21] Robinson, J., & Baker, J. E. 2000, *Mon. Not. Roy. Astron. Soc.*, 311, 781
- [22] Robinson, J., Gawiser, E., & Silk, J. 2000, *Astrophys. J.*, 532, 1
- [23] Grinstein, B., & Wise, M. B. 1986, *Astrophys. J.*, 310, 19
- [24] Matarrese, S., Lucchin, F., & Bonometto, S. A. 1986, *Astrophys. J.*, 310, L21
- [25] Dalal, N., Dore, O., Huterer, D., & Shirokov, A. 2008, *Phys. Rev. D*, 78, 123507
- [26] Matarrese, S., & Verde, L. 2008, *Astrophys. J.*, 677, L77 (MV08)
- [27] Slosar, A., Hirata, C., Seljak, U., Ho, S., & Padmanabhan, N. 2008, *J. Cosm. Astropart. Phys.*, 08, 031.
- [28] Grossi, M., Verde, L., Carbone, C., Dolag, K., Branchini, E., Iannuzzi, F., Matarrese, S., & Moscardini, L. 2009, *Mon. Not. Roy. Astron. Soc.*, 398, 321
- [29] Desjacques, V., Seljak, U., & Iliev, I. T. 2009, *Mon. Not. Roy. Astron. Soc.*, 396, 85
- [30] Pillepich, A., Porciani, C., & Oliver, H. 2010, *Mon. Not. Roy. Astron. Soc.*, 402, 191
- [31] Efstathiou, G., Frenk, C. S., White, S. D. M., Davis, M. 1988, *Mon. Not. Roy. Astron. Soc.*, 235, 715
- [32] Cole, S., Kaiser, N. 1989, *Mon. Not. Roy. Astron. Soc.*, 231, 1127
- [33] Mo, H. J., & White, S. D. M. 1996, *Mon. Not. Roy. Astron. Soc.*, 282, 347
- [34] Kaiser, N. 1984, *Astrophys. J.*, 284, L9
- [35] Percival, W. J. 2005 *Astron. Astrophys.*, 443, 819



- [36] Cooray, A., & Sheth, R. 2002, *Phys. Rep.*, 372, 1
- [37] Sheth, R. K., Mo, H. J., & Tormen, G. 2001, *Mon. Not. Roy. Astron. Soc.*, 323, 1
- [38] Sheth, R. K., & Tormen, G. 1999, *Mon. Not. Roy. Astron. Soc.*, 308, 119
- [39] Reid, B., A., et al. 2009, [arXiv:0907.1659](#)
- [40] Tegmark, M., Taylor A., Heavens A. 1997, *Astrophys. J.*, 440,22
- [41] Jungman, G., Kamionkowski, M., Kosowsky, A., Spergel, D. 1996, *Phys. Rev. D*, 54, 1332
- [42] Fisher, R. 1935, *J. Roy. Statist. Soc.*, 98, 35
- [43] Seo, H.-J., & Eisenstein, D. J. 2003, *Astrophys. J.*, 598, 720
- [44] Blake, C., & Bridle, S. 2005, *Mon. Not. Roy. Astron. Soc.*, 363, 1329
- [45] Feldman, H., A., Kaiser, N., & Peacock, J., A. 1994, *Astrophys. J.*, 426, 23
- [46] Verde, L., Peiris, H., Jimenez, R. 2006, *J. Cosm. Astropart. Phys.*, 0601, 019
- [47] Hu, W. 1998, *Astrophys. J.*, 506, 485
- [48] Larson, D., et al. 2010, [arXiv:1001.4635](#)
- [49] Komatsu, E., et al. 2009, *Astrophys. J. Suppl.*, 180, 330
- [50] Reid, B., A., Verde, L. Jimenez, R., Mena, O. 2010, *J. Cosm. Astropart. Phys.*, 01, 003
- [51] Komatsu, E., et al. 2010, [arXiv:1001.4538](#)
- [52] Riess, A., G., et al. 2009, *Astrophys. J.*, 699, 539
- [53] Kitching, T. D., Heavens, A. F., Verde, L., Serra, P., & Melchiorri, A. 2008, *Phys. Rev. D*, 77, 103008
- [54] Takada, M., Komatsu, E., & Futamase, T. 2006, *Phys. Rev. D*, 73, 083520
- [55] Takada, M. 2006, *Phys. Rev. D*, 74, 043505
- [56] Eisenstein, D., J., & Hu, W. 1997, *Astrophys. J.*, 511, 5
- [57] Lewis, A., Challinor, A., & Lasenby, A. 2000, *Astrophys. J.*, 538, 473
- [58] Geach, J. E., et al. 2009, *Mon. Not. Roy. Astron. Soc.*, 402, 1330
- [59] Orsi, A., Baugh, C. M., Lacey, C. G., Cimatti, A., Wang, Y., Zamorani G. 2009, [arXiv:0911.0669](#)
- [60] Slosar, A. 2009, *J. Cosm. Astropart. Phys.*, 03, 004
- [61] Reid, B., A., et al. 2010, in preparation
- [62] Verde, L., et al. 2002, *Mon. Not. Roy. Astron. Soc.*, 335, 432-440
- [63] White, M., Song, Y. S., and Percival, W. J. 2008, *Mon. Not. Roy. Astron. Soc.*, 397, 1348
- [64] Yadav, A. P. S., Komatsu, E., & Wandelt, B. D. 2007, *Astrophys. J.*, 664, 680
- [65] Liguori, M., & Riotto, A. 2008, *Phys. Rev. D*, 78, 123004.